

# Brain noise estimation from MEG response to flickering visual stimulation

Alexander N. Pisarchik<sup>a,b,\*</sup>, Parth Chholak<sup>a</sup>, Alexander E. Hramov<sup>b</sup>

<sup>a</sup> Center for Biomedical Technology, Technical University of Madrid, Campus Montegancedo, Pozuelo de Alarcón, Madrid 28223, Spain

<sup>b</sup> Innopolis University, 1 Universitetskaya Str., Innopolis 420500, Russia

## ARTICLE INFO

### Article history:

Received 11 February 2019

Accepted 19 February 2019

Available online 6 March 2019

### Keywords:

Brain

Cognitive neuroscience

Flickering

Frequency locking

MEG

Modulation

Noise

Phase locking

Frequency tags

## ABSTRACT

We consider the brain as an autonomous stochastic system, whose fundamental frequencies are locked to an external periodic stimulation. Taking into account that phase synchronization between brain response and stimulating signal is affected by noise, we propose a novel method for experimental estimation of brain noise by analyzing neurophysiological activity during perception of flickering visual stimuli. Using magnetoencephalography (MEG) we evaluate steady-state visual evoked fields (SSVEF) in the occipital cortex when subjects observe a square image with modulated brightness. Then, we calculate the probability distribution of the SSVEF phase fluctuations and compute its kurtosis. The higher kurtosis, the better the phase synchronization. Since kurtosis characterizes the distribution's sharpness, we associate inverse kurtosis with brain noise which broadens this distribution. We found that the majority of subjects exhibited leptokurtic kurtosis ( $K > 3$ ) with tails approaching zero more slowly than Gaussian. The results of this work may be useful for the development of efficient and accurate brain-computer interfaces to be adapted to individual features of every subject in accordance with his/her brain noise.

© 2019 The Author(s). Published by Elsevier Ltd.

This is an open access article under the CC BY license. (<http://creativecommons.org/licenses/by/4.0/>)

## 1. Introduction

All natural systems are noisy and the brain is not an exception. Inherent brain noise as known to play an important role in the nervous system. It is needed for good functionality of the brain in all levels of its organization, from neuron cells to the neural network, e.g., for signal detection and decision-making by preventing deadlocks, underlying important mechanisms of its functionality and self-organization [1–3]. Inherent brain noise is known to play an important role in brain dynamics related to perception activity [4–6] and other brain functions [7–10]. Different manifestations of brain noise were extensively studied in terms of simple stochastic processes, like the Wiener process [11–13] from the viewpoint of statistical properties [5,6,14].

The sources of brain noise can lie in random fluctuations of physiological parameters and attention. While the former arises in the neuronal network due to quasi-random release of neurotransmitters by synapses, random synaptic input from other neurons, random switching of ion channels, etc. [15,16], the latter is associated with random fluctuations of subject's attention

across trials, resulting in the variability of neuronal responses to identical stimulation [17–20]. The variability of the attentional state decreases as the strength of attention increases, i.e., attention suppresses inherent brain noise [21,22].

Many physicists and neurophysiologists highlighted positive effects of brain noise in image recognition and decision making, such as coherence resonance [7,23–27] and deadlocks prevention [1–3,28]. The former effect consists in the enhancing brain response to a weak stimulus, so that it becomes distinguishable, even when the stimulating signal is below the perception threshold [7,23], while the latter takes place in a multistable system, including a brain, where noise induces multistate intermittency, thus preventing deadlocks [2,7,28–33].

The existing experimental approaches for brain noise estimation are based on theoretical models of bistable perception [2,3]. One of the methods [2] implies the variation of a control parameter near the onset of bistability and the measurement of the hysteresis when the parameter increases and decreases. In the psychological experiment [2], the Necker cube with time-varied contrast of their inner edges was presented to a subject, who had to fix the moment of time when he/she interpreted the cube as left- or right-oriented. The hysteresis in the registered times when the contrast was increased and when it was decreased, was associated with the subject's brain noise. In another approach [3],

\* Corresponding author: Center for Biomedical Technology, Technical University of Madrid, Campus Montegancedo, Pozuelo de Alarcón, 28223 Madrid, Spain.

E-mail address: [alexander.pisarchik@ctb.upm.es](mailto:alexander.pisarchik@ctb.upm.es) (A.N. Pisarchik).

static Necker cubes with different contrasts of the inner edges were randomly presented to a subject, who had to classify the cubes as left- or right-oriented. The probability analysis of this classification allowed the estimation of the subject's brain noise. Although these methods are very powerful and provide a relatively high statistical accuracy, they are model-dependent. The development of new, model-independent experimental approaches for quantitative measurements of brain's stochastic properties could open new opportunities for studying brain functionality and even for diagnostics of some pathologies.

In this work, we consider the possibility for estimating brain noise by analyzing brain response to flickering visual stimuli. It should be noted that flickering images have attracted much attention at the beginning of the 20th century after the discovery of cinematography and television, with regard to the phenomenon *flicker fusion*. The flicker fusion appears when visual stimuli are consecutively presented with a relatively high frequency, so that the observer perceives the series of static images as a continuous movement. The biological origin of this stroboscopic effect lies in the retina memory properties to retain an image for 20–200 ms after its removal. The critical flicker frequency, i.e., the minimal frequency at which images appear continuously, depends on many external factors, such as brightness, color, size, background luminance, etc [34]. Neurophysiological data obtained in humans and monkeys show that flickering with frequency above the critical flicker fusion threshold can nevertheless cause cortical and sub-cortical visual reactions. This means that temporal integration not only occurs at the retina level, but also appears in the brain [35]. Although there were discussions in the past about the involvement of brain regions in flickering and therefore in perception binding, many researchers unanimously considered at least the involvement of occipital lobe [36–39].

When studying the brain response to flickering stimuli, many researchers deal with visual evoked potentials (VEP) or visual evoked fields (VEF). These are electrical or magnetic neural responses recorded from the surface of the scalp using electroencephalography (EEG) or magnetoencephalography (MEG), respectively. These responses are locked to repeated presentations of a visual stimulus. If the stimulus frequency is fast enough to prevent the evoked neural activity from returning to a base line state, the elicited response is continuous and called steady-state visual evoked potential (SSVEP) or steady-state visual evoked field (SSVEF). Regan [40] showed that SSVEP is almost sinusoidal at the double flicker frequency if the stimulus is pattern-reversal (image) and at the first harmonic if the stimulus is not structured (flash when eyes are closed).

As any sinusoidal wave, SSVEP/F is characterized by its amplitude and phase. The amplitude can be measured from the power spectrum, while the phase is partially locked to the flicker signal and fluctuates around its mean value. SSVEP/F offers certain advantages over the transient VEP/F for studying sensory and cognitive processes because the signal can be easily extracted from background noise and quantified [40]. Therefore, it is surprising that only a few studies attempted to relate SSVEP parameters to cognitive processes [41–43].

The majority of perception studies using flickering images were based on EEG data. Only a few papers were devoted to the MEG research, despite its higher spatial resolution. The existing MEG studies are mainly focused on binocular rivalry [36,44,45], the binding problem [46,47], and the reaction time [46,48]. For example, in the binocular rivalry experiments [44,45], the authors measured SSVEFs at different frequencies when two images with distinct frequencies were presented to each eye. The frequency-tagged MEG signals were also used for studying perception of ambiguous images [49] and cortical auditory processing [50].

Recently, the interest to visual flickering has significantly increased due to the development of SSVEP-based brain-computer interfaces (BCIs). Starting from the Vidal's work in 1973 [51], the SSVEP-based BCIs explore flickering targets with unique stimulation frequencies [52], phases [53], or combinations of both [54]. The EEG signals recorded in the occipital cortex exhibited characteristics of the gazed target, while the SSVEP amplitude was expected to be modulated by attention [55].

In this paper, we propose a new experimental approach for brain noise estimation, which is based on frequency locking of the brain response to a periodically modulated visual stimulus. As known from the theory of coupled oscillators [30], the frequency locking appears in a stochastic or a chaotic system subjected to a periodic external force. Depending on both the forcing strength and noise, the frequency locking can be either permanent or intermittent. In the intermittency regime, the time intervals of frequency locking are interrupted by unlocked periods when the phase is shifted to  $2\pi n$  radians ( $n = \pm 1, \pm 2, \dots$ ). In the frequency-locking regions, the phase of oscillations is not completely locked, but fluctuates around its mean value due to noise. The stronger the noise, the larger the fluctuations. Here, we suggest the fluctuation amplitude to be used as an indicator of internal brain noise.

## 2. Experiment

### 2.1. Experimental setup

Brain magnetic fields were recorded in a magnetically shielded room with a whole-head Vectorview MEG system (Elekta AB, Stockholm, Sweden) with 306 channels (102 magnetometers and 204 planar gradiometers). The system was placed inside a magnetically shielded room (Vacuum Schmelze GmbH, Hanau, Germany) at the Laboratory of Cognitive and Computational Neuroscience, Center for Biomedical Technology, Technical University of Madrid, Spain. Fastrak digitizers (Polhemus, Colchester, Vermont) were used to obtain the three-dimensional head shape. Three fiducial points (nasion, left and right preauricular) and more than 300 points on the scalp were acquired for each subject. A vertical electrooculogram was placed to capture blinks and other undesirable eye movements. Data were sampled at 1000 Hz with an online anti-alias bandpass filter between 0.1 Hz and 330 Hz.

### 2.2. Subjects

Eight healthy subjects (aged 23–64 years, 5 males and 3 females) with normal or corrected-to-normal vision participated in the experimental study. All subjects provided a written informed consent before the commencement of the experiment. The experimental studies were performed in accordance with the Declaration of Helsinki.

### 2.3. Visual stimuli

The visual stimulus was a gray square image on a black background generated by a personal computer on a computer monitor with a 60-Hz frame rate and projected by a digital light processing projector onto a translucent screen located 150 cm from the subjects. The pixels' brightness was modulated with either 6.67 Hz (60/9) or 8.57 Hz (60/7) frequency by a sinusoidal or a rectangular signal. The modulation depth was 100% with respect to the medium grayscale level of the pixels' brightness (128 in an 8-bit format), i.e., the image brightness was varied from completely black (0) to completely white (255). These particular modulation frequencies were chosen in preliminary experiments with other possible flicker frequencies, integer fractions of the 60 Hz frame

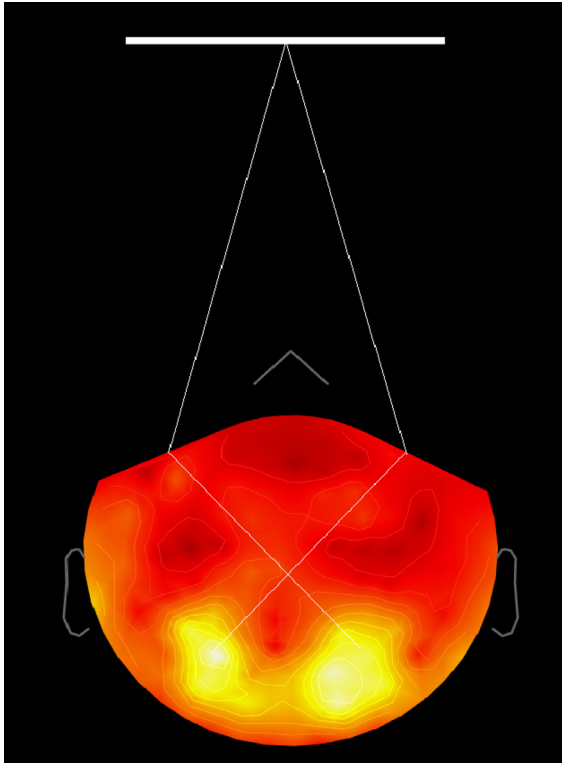


**Fig. 1.** Schematic of the experiment and coherent brain response. The subject observed a flickering image by both eyes focused on the dot on the screen.

rate (i.e., 60/2, 60/3, 60/4, 60/5, 60/6, ...), as frequencies which produce the best tagging response in the brain at the same frequencies and their higher harmonics.

The experimental design is shown in Fig. 1. The strongest signal was registered in the occipital cortex.

#### 2.4. Experimental procedure

A subject was sat in a comfortable reclining chair with his/her legs straight and arms resting on an armrest in front of them. The participant was asked to take his/her shoes off before the experiment. The experiment began with recording a two-minute activity while the subject was focusing on a red dot in the middle of a static (non-flickering) square image. This MEG trial acted as a background reference for further measurements. After a 30 s rest, the squares flickering with frequencies 6.67 Hz and 8.57 Hz were presented for 2 min each with a 30 s rest in between. Pre-processing was performed using band-pass filtering to single out frequencies of interest in order to account for phase coding.

### 3. Results

We found that brain areas affected by the flickering are individual for every subjects and depend on the flicker frequency. The best frequency tags were found at the flickering frequencies and their higher harmonics in the occipital cortex of all subjects. In further analysis we only will use MEG data from all 42 channels in this area.

#### 3.1. Time series analysis

Fig. 2 shows SSVEF as responses to stimulus modulation by flickering signals of sinusoidal and rectangular shapes. One can see

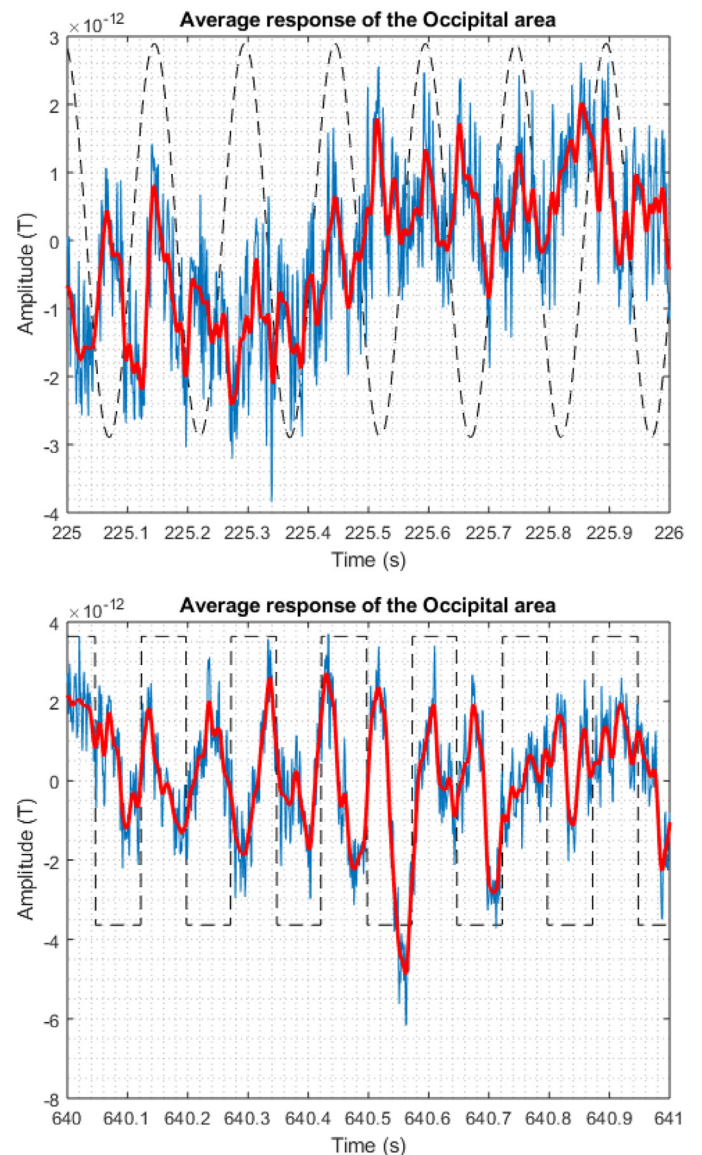


**Fig. 2.** SSVEF under 6.67 Hz stimulation of sinusoidal (upper panel) and rectangular (lower panel) shapes.

that in both cases, SSVEF is modulated at the double frequency of the stimulation. This means that the brain responds to a change in the image brightness, that is probably related to changing attention.

We found that the sinusoidal modulation induces better SSVEF signals than the rectangular modulation. Therefore, the further analysis will only be performed for the sinusoidal flickering.

In coupled stochastic or chaotic systems, noise as known [30] to result in desynchronization, that can be revealed from fluctuations of the phase difference between coupled variables. Since in our work, the higher brain response was observed at the second harmonics of the flicker frequencies, we measured the phase difference between SSVEF and the second harmonic of the flicker sinusoidal signal, as [56]

$$\Phi = (t_n^b - t_n^s)2f_s, \quad (1)$$

where  $t_n^b$  and  $t_n^s$  are the times of  $n$ th maxima of the SSVEF brain response and the second harmonic of the flicker signal, respectively, and  $f_s$  is the flicker frequency.

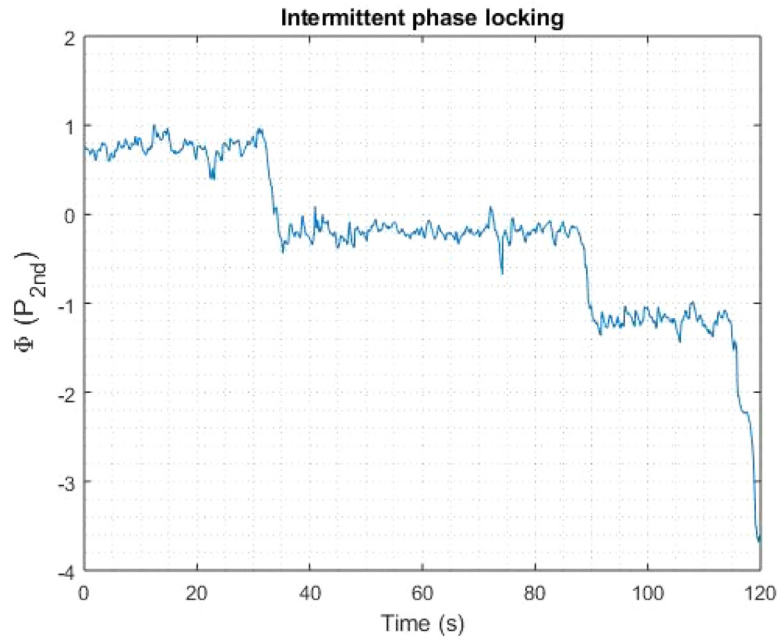


**Fig. 3.** Intermittent frequency locking. The phase  $\Phi$  fluctuates in time over a certain mean value in the frequency-locking windows and from time to time drops one or more cycles.

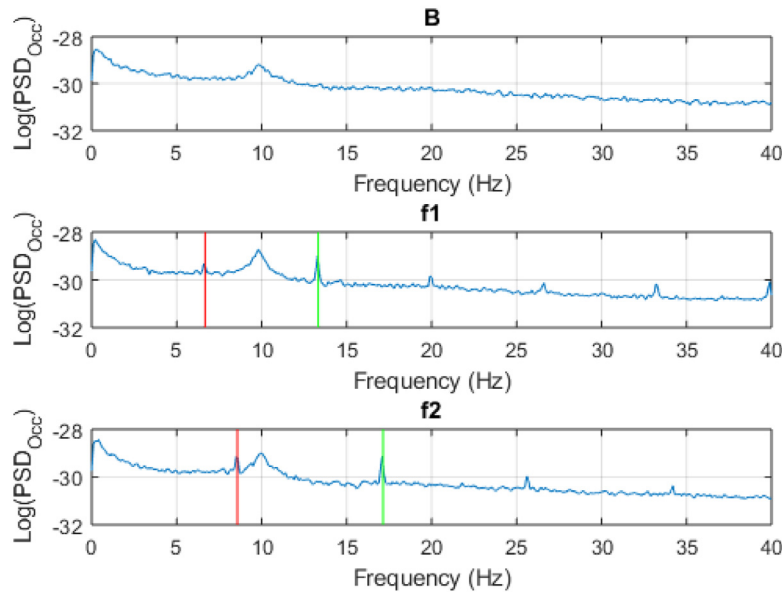


**Fig. 4.** Fourier spectra of SSVEF for the stationary image (**B**) and for the image under sinusoidal modulation at 6.67 Hz (**f1**) and 8.57 Hz (**f2**). The vertical red and green lines indicate tags at flicker frequencies and their second harmonics, respectively.

In [Fig. 3](#) we plot the time series of the SSVEF phase fluctuations  $\Phi$  in units of periods (cycles) of the second harmonic of the flicker frequency. This figure illustrates intermittent frequency locking, where the frequency is locked during certain periods of time, interrupted by unlocked intervals where  $\Phi$  drops on one or more cycles. The windows where the frequency is locked were used for the statistical analysis of the phase fluctuations.

### 3.2. Power spectrum analysis

In the frequency domain, we used the Fourier transform analysis. Since we used 2 min trials, the spectral resolution was  $1/120 = 8.3 \times 10^{-3}$  Hz.

The Fourier spectra of SSVEF in the occipital area are shown in [Fig. 4](#) for the stationary image (without flickering) (panel **B**) and with modulation at frequencies 6.67 Hz (panel **f1**) and 8.57 Hz (panel **f2**). One can see that in all spectra background noise is  $1/f$  noise (or pink noise), typical in biological systems [\[59\]](#). The broad peaks corresponding to alpha and delta waves are also seen around 10 Hz and 1 Hz, respectively. When the modulation is applied, the brain responds at the modulation frequency, as well as at its higher harmonics.

The exact tags at the flicker frequencies are shown in [Fig. 5](#).

It is noteworthy that the power of the second harmonic component is higher than the power of the first harmonic component. This means that the brain reacts on a change in the

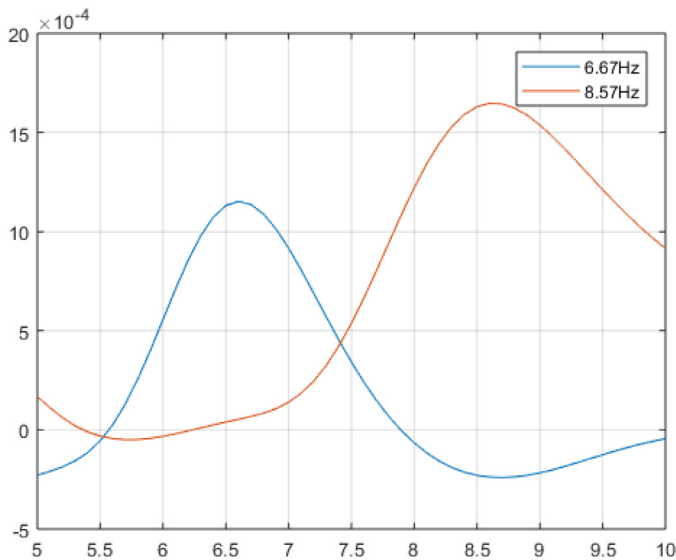


**Fig. 5.** High-resolution SSVEF power spectrum demonstrating the exact tags at 6.67 Hz (blue curve) and 8.57 Hz (red curve).

stimulus, rather than on the flicker frequency. The same is seen from the time series in Fig. 2.

The dominance of the second harmonic was also observed in the flicker experiments with binocular rivalry, which consisted in presentation of two incompatible images, one to each eye, flickered at distinct frequencies,  $f_1$  and  $f_2$ . The regions responsible for “binding” these two incompatible images into one altered perceived image show activity at the harmonics of both the tagged frequencies as well as the sum frequency. Interestingly, it was found [47] that the second harmonic component at  $2(f_1 + f_2)$  was stronger than the first harmonic at  $(f_1 + f_2)$ . The perception binding might be supported by two types of gamma oscillations in the brain, induced and evoked [57]. In addition, the higher power at the second harmonic of the flicker frequency was also highlighted by Di Russo et al. [58], who studied visual evoked potentials (VEPs) in the EEG data when stimuli were presented at a constant rate.

### 3.3. Kurtosis

Brain noise was estimated from the probability distribution of the SSVEF phase fluctuations  $\Phi$ . The time intervals corresponding to the unlocked frequency were excluded from consideration, and the time series were corrected by adding or subtracting one or more periods. The phase histograms were calculated for each subject using the SSVEF time series during the 2 min stimulus presentation, similar to those shown in Fig. 6.

The sharpness of the distributions shown in Fig. 6 is characterized by kurtosis defined as

$$K = \frac{E(\Phi - \langle \Phi \rangle)^4}{\sigma^4}, \quad (2)$$

where  $\langle \Phi \rangle$  is the average phase difference,  $\sigma$  is the standard deviation, and  $E$  is the function of the expected value. It should be noted that in some definitions of kurtosis, 3 is subtracted from the computed value in order to get a kurtosis value of 0 for normal distribution. However, in the scope of this paper, the kurtosis for normal distribution is 3.

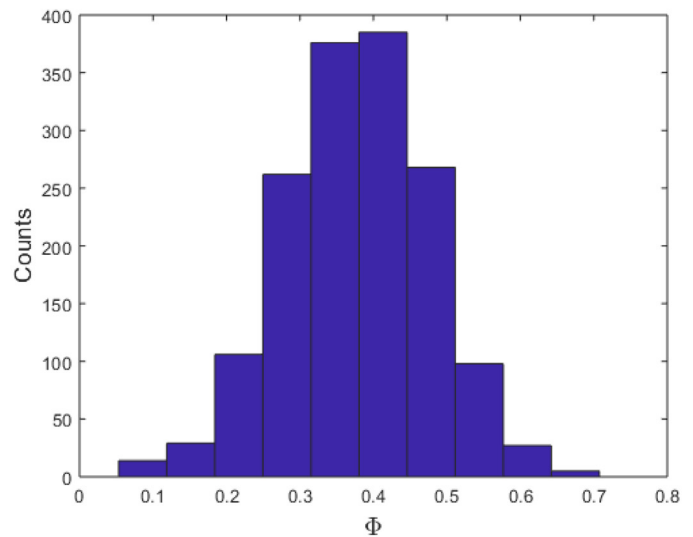
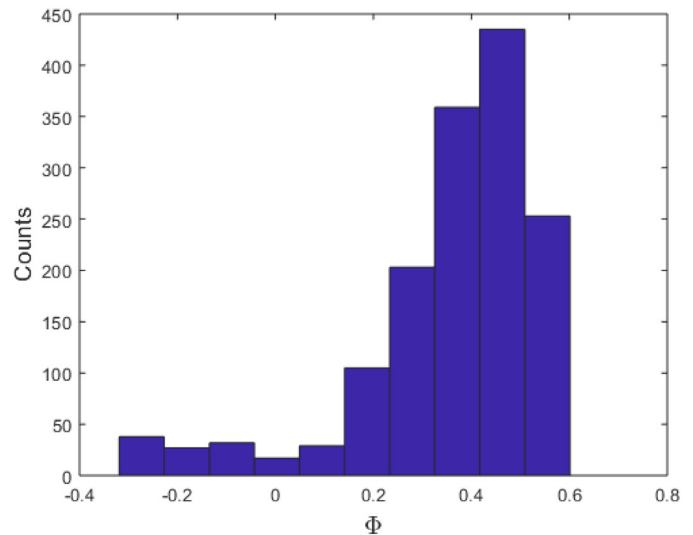


**Fig. 6.** Probability distribution of SSVEF phase fluctuations for 6.67 Hz modulation for subjects 6 (upper panel) and 4 (lower panel) exhibiting weak and strong brain noise, respectively.

Here, we assume that brain noise leads in the broadening of the phase probability distribution, and therefore it can be associated with inverse kurtosis. The stronger the noise, the wider the probability distribution. The kurtosis values for all subjects are present in Fig. 7 for 6.67 Hz ( $f_1$ ) and 8.57 Hz ( $f_2$ ) flicker frequencies. While for 6.67 Hz modulation the exact frequency tags were found in all subjects, the 8.57 Hz frequency were locked in four subjects only. Since noise is stronger at higher frequencies (see Fig. 4), since kurtosis for 8.57 Hz is smaller than for 6.67 Hz stimulation, we suppose that brain noise is stronger for 8.57 Hz.

One can see that in our experiments kurtosis varied from 3.1 to 6 for 6.67 Hz and from 2.6 to 4 for 8.57 Hz modulation among subjects. Since the kurtosis of the normal distribution is 3, the majority of subjects exhibited leptokurtic kurtosis ( $K > 3$ ), when tails approach zero more slowly than Gaussian. Only one subject (subject 5 for 8.57 Hz) had platykurtic kurtosis ( $K < 3$ ) and three subjects (subject 4 for 6.67 Hz and subjects 7 and 1 for 8.57 Hz) exhibited almost normal distributions ( $K \approx 3$ ).

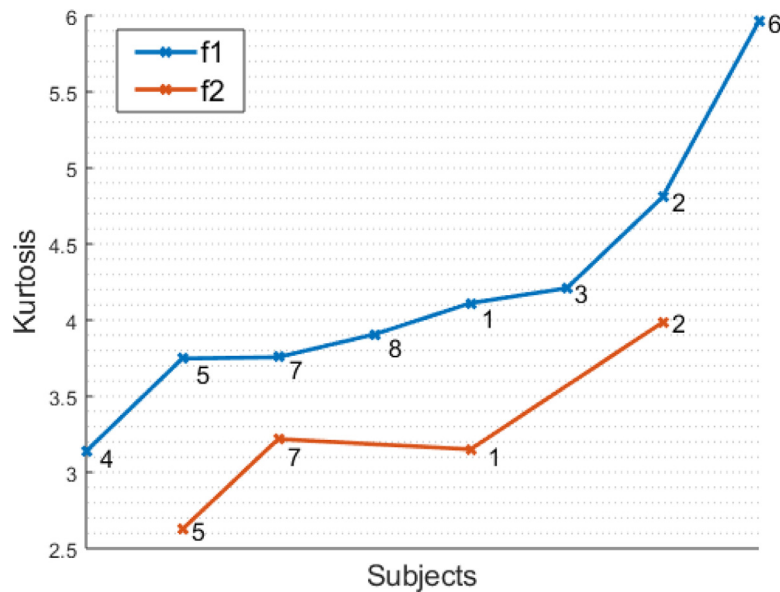


Fig. 7. Kurtosis values for all subjects for 6.67 Hz (blue curve) and 8.57 Hz (red curve) flicker frequencies.

#### 4. Conclusion

In this paper, we have proposed a novel method for experimental estimation of brain noise. A quasi-steady phase fluctuation of the brain response to the flickering visual stimulation was used to evaluate brain noise. In the MEG experiments with eight healthy subjects, the strongest brain response was observed at the second harmonic of the 6.67 Hz flicker frequency in the occipital area. The inverse kurtosis of the probability distribution of SSVEF phase fluctuations was associated with brain noise. We suppose that this noise is mainly related to neural noise arising from random neurophysiological activity of the neural network, while attention noise leads to intermittent frequency unlocking. The latter noise requires further investigation.

Since neural network is unique for each individual, the results of this work may be useful for the development of effective brain-computer interfaces which can be adopted according to subject's brain noise.

#### Acknowledgments

The authors thank the [Ministry of Economy and Competitiveness](#) (Spain) for support through the project Ref. SAF2016-80240-P for experimental research. A. E. H. acknowledges support from the [Russian Science Foundation](#) through the grant no. 17-72-30003 for data analysis.

#### References

- [1] Kelso JAS. *Dynamic patterns: the self-organization of brain and behavior*. A Bradford Book; 1997.
- [2] Pisarchik AN, Jaimes-Reátegui R, Magallón-García CDA, Castillo-Morales CO. Critical slowing down and noise-induced intermittency in bistable perception. *Biol Cybern* 2014;108:397–404.
- [3] Runnova AE, Hramov AE, Grubov VV, Koronovskii AA, Kurovskaya MK, Pisarchik AN. Theoretical background and experimental measurements of human brain noise intensity in perception of ambiguous images. *Chaos Solitons Fractals* 2016;93:201–6.
- [4] Huguet G, Rinzel J, Hupé JM. Noise and adaptation in multistable perception: noise drives when to switch, adaptation determines percept choice. *J Vis* 2014;14:1–24.
- [5] Gigante G, Mattia M, Braun J, Giudice PD. Bistable perception modeled as competing stochastic integrations at two levels. *PLoS Comput Biol* 2009;5:E1000430.
- [6] Moreno-Bote R, Rinzel J, Rubin N. Noise-induced alternations in an attractor network model of perceptual bistability. *J Neurophysiol* 2007;98:1125–39.
- [7] Andreev AV, Makarov VV, Runnova AE, Pisarchik AN, Hramov AE. Coherence resonance in stimulated neuronal network. *Chaos Solitons Fractals* 2018;106:80–5.
- [8] Kitajo K, Nozaki D, Ward LM, Yamamoto Y. Behavioral stochastic resonance within the human brain. *Phys Rev Lett* 2003;90:218103.
- [9] Prussek J, Lehnertz K. Stochastic qualifiers of epileptic brain dynamics. *Phys Rev Lett* 2007;98:138103.
- [10] Smith PL, Ratcliff R. Psychology and neurobiology of simple decisions. *Trends Neurosci* 2004;27:161–8.
- [11] Ratcliff R, Smith PL. A comparison of sequential sampling models for two choice reaction time. *Psychol Rev* 2004;111:333–67.
- [12] Heekeren HR, Marrett S, Ungerleider LG. The neural systems that mediate human perceptual decision making. *Nat Rev Neurosci* 2008;9:467–79.
- [13] Wang XJ. Neural dynamics and circuit mechanisms of decision-making. *Curr Opin Neurobiol* 2012;22:1039–46.
- [14] Merk I, Schnakenberg J. A stochastic model of multistable visual perception. *Biol Cybern* 2002;86:111–16.
- [15] Jacobson GJ, Diba K, Yaron-Jakoubovitch A, Oz Y, Koch C, Segev I, Yarom Y. Subthreshold voltage noise of rat neocortical pyramidal neurones. *J Physiol* 2005;564:145–60.
- [16] Deco G, Rolls ET, Romo R. 2009 Stochastic dynamics as a principle of brain function. *Prog Neurobiol* 2009;88:1–16.
- [17] Cohen MR, Maunsell JHR. A neuronal population measure of attention predicts behavioral performance on individual trials. *J Neurosci* 2010;30:15241–53.
- [18] Cohen MR, Maunsell JHR. Using neuronal populations to study the mechanisms underlying spatial and feature attention. *Neuron* 2011;70:1192–204.
- [19] Denfield GD, Ecker AS, Shinn TJ, Bethge M, Tolias AS. Attentional fluctuations induce shared variability in macaque primary visual cortex. *Nat Commun* 2018;9:2654.
- [20] Maksimenko VA, Hramov AE, Frolov NS, Lüttjohann A, Nedaivozov V, Grubov VV, Runnova AE, Makarov VV, Kurths J, Pisarchik AN. Increasing human performance by sharing cognitive load using brain-to-brain interface. *Front Neurosci* 2018;12:949.
- [21] Ecker AS, Denfield GH, Bethge M, Tolias AS. On the structure of neuronal population activity under fluctuations in attentional state. *J Neurosci* 2016;36:1775–89.
- [22] Rabinowitz NC, Goris RL, Cohen M, Simoncelli EP. Attention stabilizes the shared gain of v4 populations. *Elife* 2015;4:e08998.
- [23] Simonotto E, Riani M, Seife C, Roberts M, Twitty J, Moss F. Visual perception in stochastic resonance. *Phys Rev Lett* 1997;78:1186–9.
- [24] Toral R, Mirasso CR, Gunton JD. System size coherence resonance in coupled Fitzhugh–Nagumo models. *Europhys Lett* 2003;61:162–7.
- [25] Pisarchik AN, Jaimes-Reátegui R. Deterministic coherence resonance in coupled chaotic oscillators with frequency mismatch. *Phys Rev E* 2015;92:050901(R)1–5.
- [26] Yilmaz E, Ozer M, Baysal V, Perc M. Autapse-induced multiple coherence resonance in single neurons and neuronal networks. *Sci Rep* 2016;6:30914.
- [27] García-Vellisca MA, Pisarchik AN, Jaimes-Reátegui R. Experimental evidence of deterministic coherence resonance in coupled chaotic systems with frequency mismatch. *Phys Rev E* 2016;94:012218.
- [28] Hramov AE, Frolov NS, Maksimenko VA, Makarov VV, Koronovskii AA, García-

- Prieto J, Antón-Toro LF, Maestú F, Pisarchik AN. Artificial neural network detects human uncertainty. *Chaos* 2018;28:033607.
- [29] Pisarchik AN, Feudel U. Control of multistability. *Phys Rep* 2014;540:167–218.
- [30] Boccaletti S, Pisarchik AN, del Genio CI, Amann A. Synchronization: from coupled systems to complex networks. Cambridge Univ Press; 2018.
- [31] Hramov AE, Pchelintseva SV, Runnova AN, Musatov VY, Grubov VV, Zhuravlev MO, Maksimenko VA, Koronovskii AA, Pisarchik NN. Classifying the perceptual interpretations of a bistable image using EEG and artificial neural networks. *Front Neurosci* 2017;11:674.
- [32] Maksimenko VA, Runnova AE, Zhuravlev MO, Makarov VV, Nedayvozov V, Grubov VV, Pchelintseva SV, Hramov AE, Pisarchik AN. Visual perception affected by motivation and alertness controlled by a noninvasive brain-computer interface. *PLoS One* 2017;12:e0188700.
- [33] Pisarchik AN, Bashkirtseva I, Ryashko L. Stochastic sensitivity of a bistable energy model for visual perception. *Ind J Phys* 2017;91:57–62.
- [34] Landis C. Something about flicker-fusion. *Sci Mon* 1951;73:308–14.
- [35] Di Lollo V, Bischof WF. Inverse-intensity effect in duration of visible persistence. *Psychol Bull* 1995;118:223–37.
- [36] Cosmelli D, David O, Lachaux JP, Martinerie J, Garnero L, Renault B, Varela F. Waves of consciousness: ongoing cortical patterns during binocular rivalry. *Neuroimage* 2004;23:128–40.
- [37] Engel AK, Singer W. Temporal binding and the neural correlates of sensory awareness. *Trends Cogn Sci* 2001;5:16–25.
- [38] Shadlen MN, Movshon JA. Synchrony unbound: a critical evaluation of the temporal binding hypothesis. *Neuron* 1999;24:67–77.
- [39] Varela F, Lachaux JP, Rodriguez E, Martinerie J. The brainweb: phase synchronization and large-scale integration. *Nat Rev Neurosci* 2001;2:229–39.
- [40] Regan D. Human brain electrophysiology: evoked potentials and evoked magnetic fields in science and medicine. Elsevier; 2002.
- [41] Wilson GF, O'Donnell RD. Steady-state evoked responses: correlations with human cognition. *Psychophysiol* 1986;23:57–61.
- [42] Silberstein RB, Schier MA, Pipingas A, Ciorciari J, Wood SR, Simpson DG. Steady-state visually evoked potential topography associated with a visual vigilance task. *Brain Topogr* 1990;3:337–47.
- [43] Müller MM, Teder-Sälejärvi AW, Hillyard SA. The time course of cortical facilitation during cued shifts of spatial attention. *Nat Neurosci* 1998;1:631–4.
- [44] Tononi G, Srinivasan R, Russell DP, Edelman GM. Investigating neural correlates of conscious perception by frequency-tagged neuromagnetic responses. *Proc Natl Acad Sci* 1998;95:3198–203.
- [45] Kamphuisen A, Bauer M, Van Ee R. No evidence for widespread synchronized networks in binocular rivalry: MEG frequency tagging entrains primarily early visual cortex. *J Vis* 2008;8:4.
- [46] Amano K, Goda N, Nishida S, Ejima Y, Takeda T, Ohtani Y. Estimation of the timing of human visual perception from magnetoencephalography. *J Neurosci* 2006;26:3981–91.
- [47] Aissani C, Cottureau B, Dumas G, Paradis AL, Lorenceau J. Magnetoencephalographic signatures of visual form and motion binding. *Brain Res* 2011;1408:27–40.
- [48] Ruhnau R, Keitel C, Lithari C, Weisz N, Neuling T. Flicker-driven responses in visual cortex change during matched-frequency transcranial alternating current stimulation. *Front Hum Neurosci* 2016;10:184.
- [49] Parkkonen L, Andersson J, Hämmäläinen M, Hari R. Early visual brain areas reflect the percept of an ambiguous scene. *Proc Natl Acad Sci* 2008;105:20500–20504.
- [50] Lamminmäki S, Parkkonen L, Hari R. Human neuromagnetic steady-state responses to amplitude-modulated tones, speech, and music. *Ear Hear* 2014;35:461–7.
- [51] Vidal JJ. Toward direct brain-computer communication. *Annu Rev Biophys Bioeng* 1973;2:157–80.
- [52] Middendorf M, McMillan G, Calhoun G, Jones KS. Brain-computer interfaces based on the steady-state visual-evoked response. *IEEE Trans Rehabil Eng* 2000;8:211–14.
- [53] Manyakov NV, Chumerin N, Van Hulle MM. Multichannel decoding for phase-coded SSVEP brain computer interface. *Int J Neural Syst* 2012;22:1250022.
- [54] Jia C, Gao X, Hong B, Gao S. Frequency and phase mixed coding in SSVEP-based brain computer interface. *IEEE Trans Biomed Eng* 2011;58:200–206.
- [55] Kelly SP, Lalor EC, Reilly RB, Foxe JJ. Visual spatial attention tracking using high-density SSVEP data for independent brain-computer communication. *IEEE Trans Neural Sys Rehabil Eng* 2005;13:172–8.
- [56] Pisarchik AP, Jaimes-Reategui R, Villalobos-Salazar JR, García-López JH, Boccaletti S. Synchronization of chaotic systems with coexisting attractors. *Phys Rev Lett* 2006;96:244102.
- [57] Martinovic J, Busch NA. High frequency oscillations as a correlate of visual perception. *Int J Psychophysiol* 2011;79:32–8.
- [58] Di Russo F, Teder-Sälejärvi WA, Hillyard SA. Steady-state VEP and attentional visual processing. The cognitive electrophysiology of mind and brain. Elsevier; 2002.
- [59] Szendro P. Pink-noise behaviour of biosystems. *Eur Biophys J* 2001;30:227–231.